Advances in Science and Technology, Vol. 11, No. 2, September / October 2017, pp 72 - 84

Geophysical Analysis of Badia Canal Region in Lagos, Nigeria, Using the Ground Penetrating Radar

B.I. Ijeh[1,2*], N.E. Enyioko[1] and M.E. Emetere [2]

[1]Department of Physics, Michael Okpara University of Agriculture, Umudike, Abia State.

[2]Department of Physics, Covenant University, Ota, Nigeria.

(Submitted: August 13, 2017; Accepted: October 15, 2017)

Abstract

The Badia canal region is within the deserted shoreline edge complex. The area is low lying and elevation ranges from 0.54 m to about 3.2 m above mean sea-level. Ground Penetrating Radar (GPR) technique was adopted under some specific measurement design to obtain the subsurface lithology, geophysical and engineering parameters that will guide the sub-structural design. Eight traverses were carried-out. All traverses were 530 m long and ran from land (marshy) to water, with traverse-traverse separation of 2.5 m. A 16-overlap stack was utilized for the traces amid information recording to enhance the signal to noise(s/n) proportion of the information. The GPR information situating was aligned utilizing a review wheel (odometer) and every radar trace contains 1024 points/focuses per trace. A velocity value of 0.13 m ns^{-1} was obtained from the velocity spectrum analysis of the GPR sections. Derived parameters from the GPR studies shows that the Peat found in the investigated area at Badia are fibrous peat with low strength, medium to low bedding stress and high volumetric water content (VWC). Good correlation exists between the geophysical properties estimated from the GPR data and the field data obtained.

Keywords: Lithologic, Badia canal region, ground penetrating radar, electromagnetic wave.

1.0 Introduction

In modern practice, Ground Penetrating Radar (GPR) method is routinely used to effectively map the spatial variation of soil and rock layers with its thickness. GPR is environmentally friendly, a safe and non-destructive technique that creates a nonstop cross-sectional profile or record of the coveted subsurface components, without penetrating, examining, or burrowing. It can be used in assessing roads, railways, bridges, airport, tunnels and environmental objects (Saharudin *et al.,* 2016; Timo and Pekka, 2011). It is a relatively new geophysical technique (Doolittle, 2013). GPR has been widely used in developed countries to investigate rock properties beneath the earth. Ground penetrating radar performs well with rocks than on water. Rocks have low electric conductivity and low attractive penetrability. In rocks containing conductive minerals, the infiltration of the radar wave is typically confined because of the electromagnetic properties of the desired rock-type. The entrance of the flag and the recognition determination of GPR depend essentially on the recurrence of the radio wire utilized. By and large, the reception apparatus of higher recurrence give better location of individual targets yet the weakening of the flag is additionally more grounded, giving less infiltration in the rock.

GPR transmits a beat electromagnetic wave from a transmitter and signs are gotten by an accepting reception apparatus. The transmitted signal proliferates through the subsurface material and is reflected by earth crust constituents to give a specific imagery. The captured images from simulation may reveal the location of the anomaly and perhaps some indication of depth of burial and lateral extent (Oldenburg and Pratt, 2007). Aside the geosciences (Annan, 2002), GPR have shown wide application in diverse fields' e.g. agronomy, archaeology, engineering, environmental assessment, and underground investigations. For this study, GPR was used to carry out stratigraphic survey across the Badia canal area with a view to providing the subsurface lithology, geophysical and engineering parameters that will guide the sub-structural design and construction of the proposed drainage channel.

*Corresponding Author's E-mail Address: bonijeh@gmail.com

Leggo and Leech (1983) reported the use of GPR on voids and cavities exploration. Neal (2004) explored the use of GPR on the depth of water table. Patterson (2001) demonstrated that the GRP technique was successfully used to explore gem tourmaline pockets and vugs. Van Dam *et al.* (2003) applied GPR to investigate geological structures hosting mineral deposits and reported a successful exploration of iron oxide deposits with the GPR. Doolittle, *et al.* (2008) conducted thematic mapping (with GPR) to investigate the relative suitability of soils for GPR applications inside similarly extensive territories of the United States. Leuschen *et al.* (2001) outlined the advancement of a lightweight, low power, ground-entering radar framework expected for the subsurface investigation of Mars. He considered the reproduction and plan of a GPR framework to test the Martian subsurface for fluid layers in either fluid or strong state. He accepted that a fundamental stride in planning such a framework is to reenact the radar reactions from geophysical models in view of what could be normal on Mars.

Furthermore, Takahashi (2011) applied two experiments of GPR measurements and analyses to monitor irrigation with intention to demonstrate the ability of GPR to measure and monitor changes in the soil water content. The first experiment analyzes reflections at the soil surface and the second, a measurement of correlation between boreholes. After irrigation, GPR measurements were tested to see its capability in monitoring the changes in soil dielectric properties and their spatial variation. The Badia canal region is within the abandoned beach ridge complex. The area is low lying and elevation ranges from 0.5 m to about 3.0 m above mean sea-level. The peculiarity of the geological settings requires the combination of selected technique of the GPR measurement. The main objective of the research is to validate the GPR method in a complex geological terrain. Datasets, which are the reflection profiles, and with some minor filtering, are used to create amplitude slice-maps, which are often considered acceptable final products (Goodman and Piro, 2013). Other image production products are the creation of isosurface renderings of buried materials or videos of the ground produced in a number of orientations, usually produced after the production of the slice-maps (Conyers, 2015).

1.1 The Study Area

Geographically, the study area is bounded by latitude 7.15 ^{0}N and 7.16 ^{0}N, and longitude 5.386 ^{0}E and 5.403 ^{0}E, and spans about 55.07 hectares. The study area lies within the Dahomey basin which constitutes a part of the post-Hercynian margin-sag basins of West Africa (Figure 1). The study area contains underlying formations of solid matter derived from organisms, organic materials derived peat. Peat is partially decomposed remains of dead plants which have been accumulated under water for thousands of years (Huat *et al*, 2009). The Badia area is within the abandoned beach ridge complex. The area is low lying and elevation ranges from 0.5 m to about 3.4 m above mean sea-level. The area lies within the rain forest zone of Nigeria with mean annual rainfall of above 1500 mm.

Physically, the whole zone is swampy with sand filling in separated ranges for development of residences. The study range is not depleted. Amid dry season, water level is around 300 mm subterranean levels in up to 70% of the whole review region while some are beneath ocean level (Apapa Local Government, 2002). Amid wet season, the entire range is submerged in surge for over three hours after each rain with a few territories remaining completely submerged all through the whole wet season.

The surface neighborhood geography of the review zone is steady with the territorial topographical setting of Lagos range as portrayed by Longe, *et al*., (1987). The surface geology of the review territory is comprised of both the Ilaro and Benin Formations. The neighborhood subsurface topography is comprised of the Benin development (Miocene to Recent) and the current littoral alluvial stores (Jones and Hockey, 1964). The Benin arrangement comprises of thick collections of yellowish (ferruginous) and white sand. It is friable, inadequately sorted with intercalations of shale, dirt focal points and sandy mud with lignite. The geography guide of the territory is shown in Figure 2.

The Ilaro Formation comprises of rather gigantic sandstone with nearby earth intercalations. The Ilaro Formation extends from fine to medium grain that is genuinely very much sorted. The Ilaro Formation lies comparably on the Oshosun Formation (Lower – Middle Eocene) and locally unconformable un-

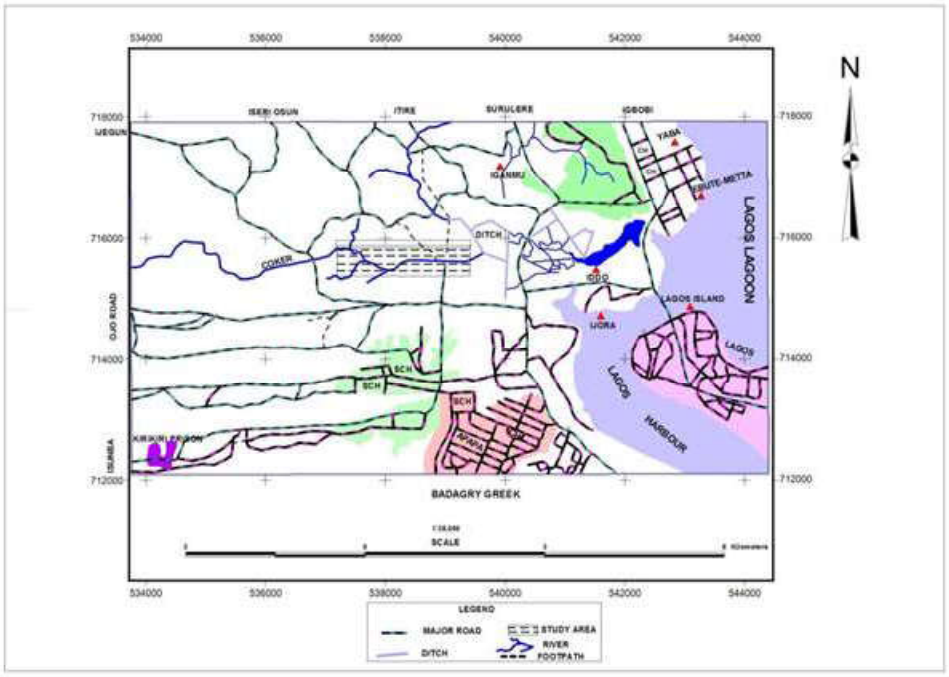

Figure 1: Location Map of the Study area.

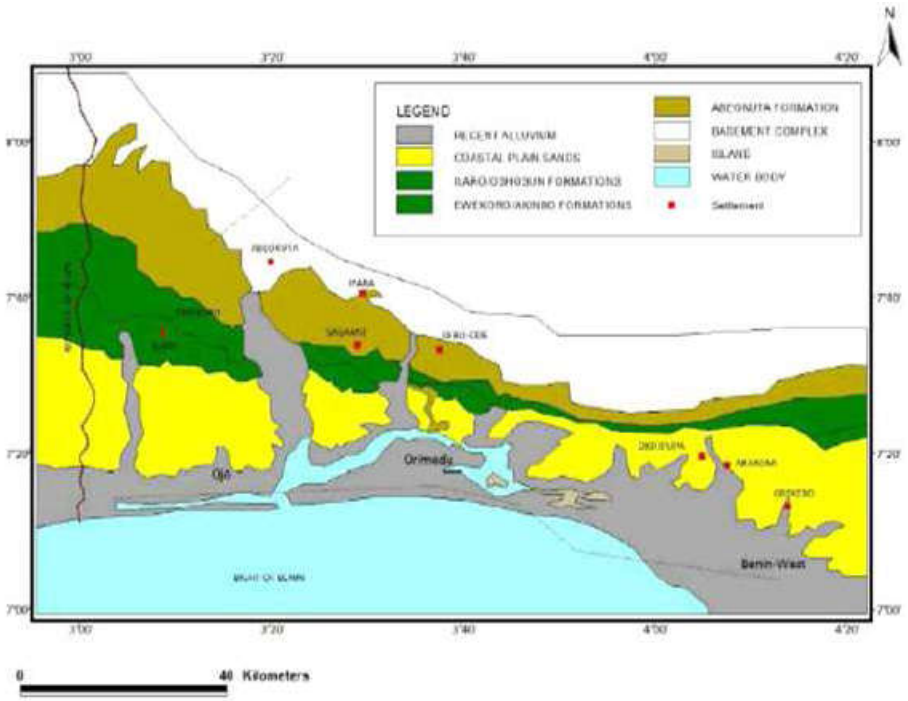

Figure 2: Geological Map of Eastern Dahomey Basin (Modified after Agagu (1985)

derneath the Benin Formation (Oligocene-Pleistocene). The Ilaro Formation is evaluated to be around 70 m thick and shows quick parallel facies changes. The Ilaro Formation is for the most part prone to be Middle to Upper Eocene in age (Figure 3).

The Benin Formation comprises mainland sands with shale intercalations as a rule with great ground water potential. This can influence the aquifer nature of the Ilaro Formation (Durotoye, 1975). Be that as it may, the hidden Ewekoro Formation is known to have great groundwater aquifer (limestone). The Ewekoro Formation is comprised of limestone while Ilaro and Benin formations are dominatingly coarse sandy estuarine, deltaic and

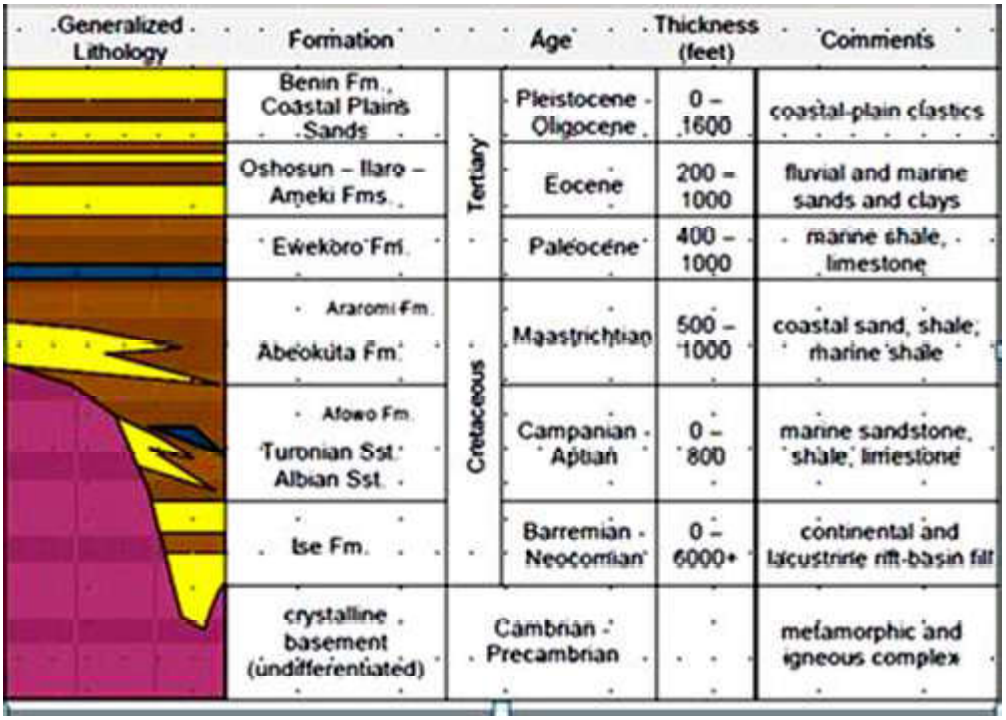

Figure 3: Stratigraphy of the Dahomey Basins showing the Formation found in Lagos, Lagos State (Jones and Hockey, 1964).

mainland beds (Olabode and Mohammed, 2016).The groundwater level changes between 1 m and 2 m. The water-bearing aquifers comprise sands, rock or a blend of the two. Textural varieties from fine through medium to coarse sands and rock happen and they are inadequately sorted. At the point when close to the surface, the sand stores are by and large free yet turn out to be decently thick with profundity and infrequently with clay interbeds (Longe *et al*, 1987). The area is well suited for water supply through boreholes.

2.0 Materials and Methods

For this study, GPR data were acquired along eight (8) parallel traverses approximately East-West, using the Geophysical Survey System Incorporated SIR system-3000 equipment. However, the area of interest covers four (4) parallel traverses. The study was done utilizing a 200 MHz monostatic protected receiving wire situated parallel to the review course (parallel-broadside) in persistent gathering mode. The radio wire was preset with three pick up focuses keeping in mind the end goal to enhance the sweeps amid information securing while thirty-three (33) checks per meter were taken (speaking to 3 cm station dispersing) with a testing window of 400 ns with counterbalance of +25 ns. A 16-overlay stack was utilized for the traces amid information recording to enhance the signal to noise (s/n) proportion of the information. The GPR information situating was aligned utilizing a study wheel (odometer) and every radar trace contains 1024 points/focuses per follow. GPR data were acquired both on land and water. The SIR-system and antenna were pulled manually on land during data collection while they were mounted on a wooden boat during data collection on water. All traverses were 530 m long and ran from land (marshy) to water, with traverse-traverse separation of 2.5 m (Figure 4).

Two kinds of processing; basic and advanced processing were applied to the acquired GPR data. The basic processing structure include; data editing (which involves data reorganization, data file merging, data header background information updates, inclusion of topography information in every file), zero-offset correction, dewowing, band-pass filtering (with a centre frequency of 200 MHz and cutoff frequencies of 100 MHz and 300 MHz), filtering in wavenumber domain and application of gain functions (Neal, 2004).

The intended effect of the deconvolution process was to remove the ringing multiples associated with water layers. The attribute analyses were generated by Hilbert transformation functions, which include instantaneous frequency, instantaneous phase and instantaneous amplitude. A velocity value of 0.13 m ns^{-1} was obtained from the velocity spectrum analysis of the GPR sections and it was used for the time-depth conversion of the data. The flow chart of the GPR processing steps used in this study is shown in Figure 4.

3.0 Results and Discussion

The depth of penetration of the radar signals range from 22 m to 24 m in the studied area. The results obtained from the processed GPR data are interpreted stratigraphically in terms of the radar facies, in correlation with the borehole logs obtained in the area and with empirical equations to infer the in-situ engineering characteristics of the peat bog. Figure 5 shows the contoured map of the peat thicknesses. An obvious decrease in depth to the peat vis-à-vis peat thicknesses from Ch.625 m to Ch.1100 m was obtained from this study. Figure 6 shows the depth to the Peat layer obtained at every 25m commencing at Ch.625 m to 1100 m, referenced to Canal centre line obtained from this study. These values were then plotted against the traverse width of 20m. The process was repeated for Ch.650 to Ch. 1100m. An obvious increase in depth to the Peat from Traverse 1 to 8 is evident. The stratigraphic cross-sections obtained at every 25m across Traverses T1 to T8 were obtained from plates 1 to 20.

The stratigraphic interpretation of the GPR sections is done in terms of radar facies for all the traverses. The radar facies observed defines the vertical profile as well as the architectural element - scale features described and interpreted in the borehole logs. The facies are defined using the basic principle of seismic interpretation techniques on the basis of reflection amplitude, continuity and configuration (Mitchum *et al*., 1977).

Five radar facies were recognized from the GPR sections. These are named: F1, F2, F3, F4 and F5. F1 is interpreted as the top soil/sand-filled area. Its thickness ranges between 0 m and 1.5 m and varies (the thickness is not constant even within the same radar profile). F2 has thickness ranges between 9m and 14m and varies (the thickness is not constant even within the same radar profile). It is interpreted as silt-clay. The thickness of F3 ranges between 2 m and 5 m and varies (the thickness is not constant even within the same radar profile). It is interpreted as peat. F4 and F5 are characterized by sub-parallel sinuous (at the upper portion) and wavy (toward the bottom of the radar) reflections, moderately amplitude reflections. This radar facies is interpreted as layer of sandy clay (F4) and silt-sand (F5).

The trial traverse is shown in Figure 7. The radar facies that characterize the first traverse are F1, F3, F5 and F4 (Figure 8). The depth to the water table on is 1 m. The depth of the peat layer ranges from 2 m to 6 m and the thickness of the peat range from 4 m to 8 m. The lithologic units that occur on the traverse are topsoil, peat, sandy clay and silt sand.

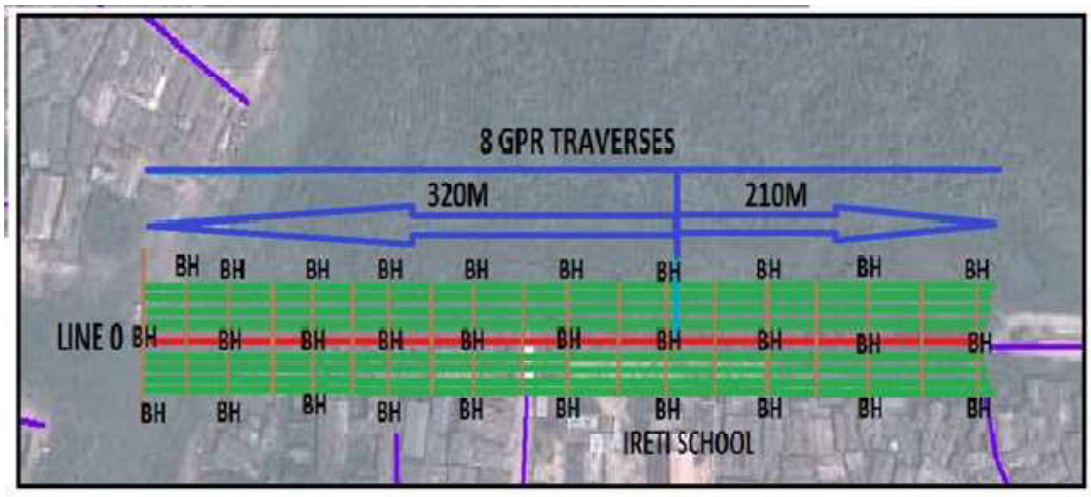

Figure 4**:** Google earth image of the study area showing the GPR traverses and the Borehole Locations.

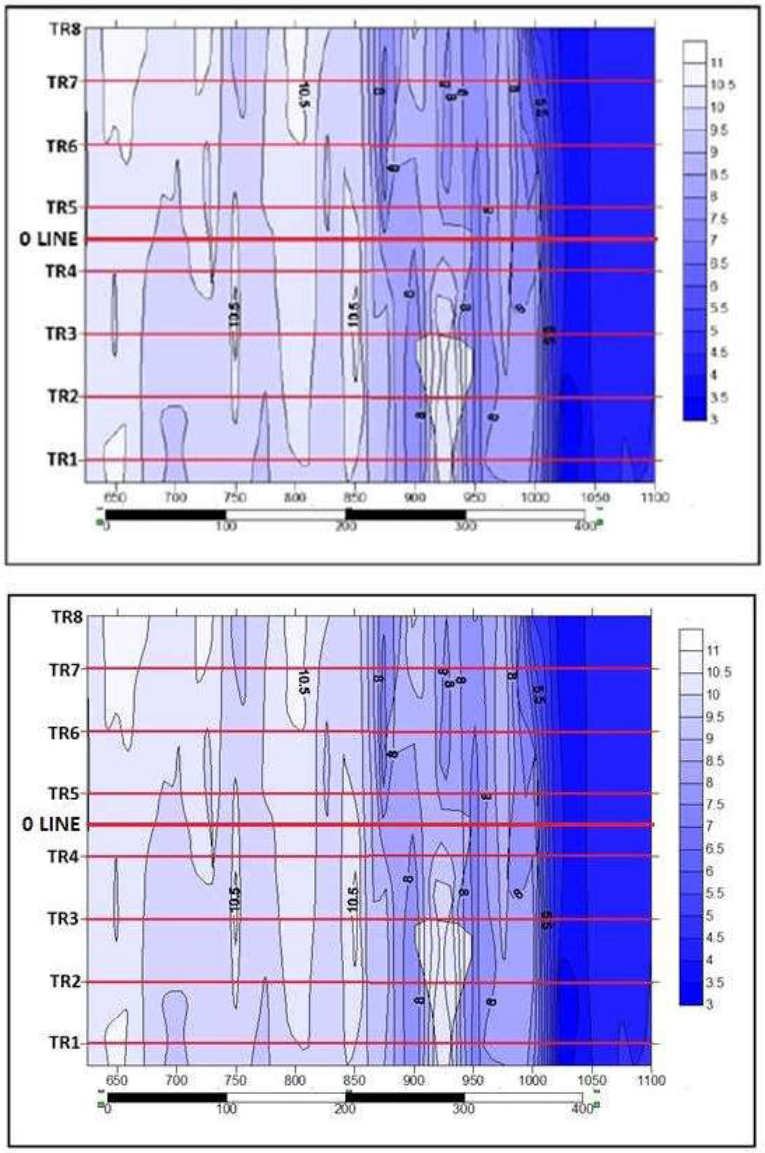

Figure 5: The Contoured map of the Peat Thicknesses (metres) using the Eight Traverses commencing at Ch.625 m to Ch.1100 m.

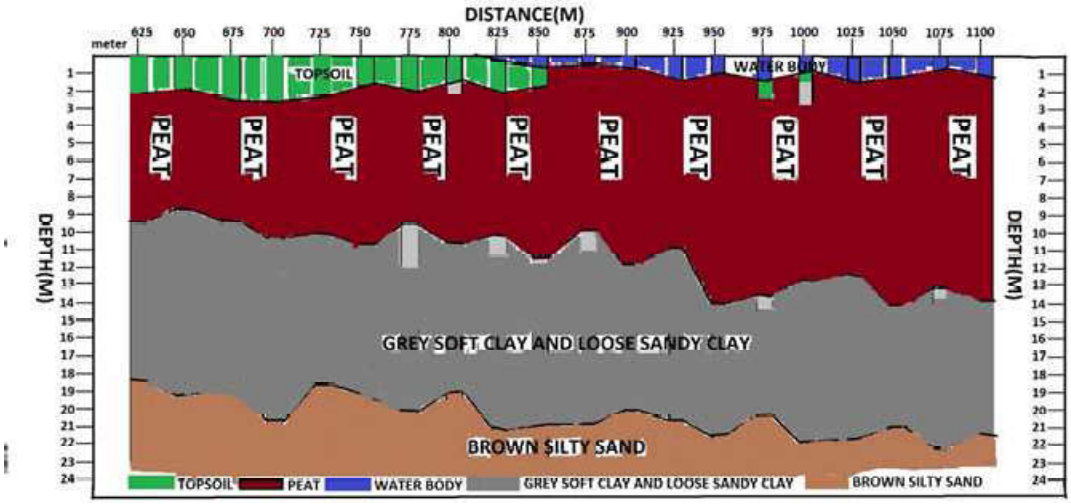

Figures 6: Stratigraphic Cross section from Ch.625 m – Ch. 1100 (LINE 0).

A borehole (BH 03) was drilled along the traverse and the result of the log interpretation is presented in Figure 9.

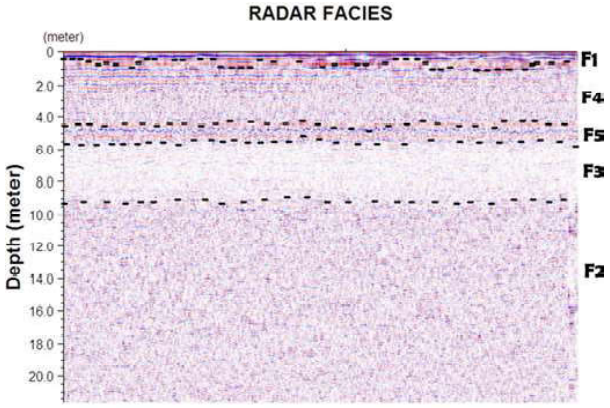

Figure 7: Radar facies identified in GPR sections

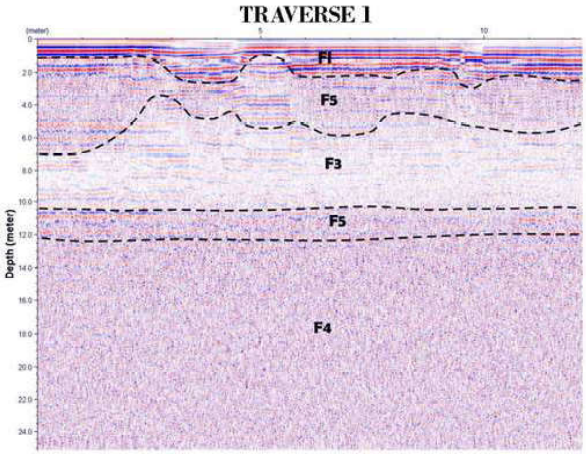

Figure 8: Radar facies for Traverse 1

The radar facies that characterize the second traverse are F4, F5, F3 and F2 (Figure 10). The depth to the water table on is 0 m. The depth of the peat layer ranges from 6 m to 6.5 m and the thickness of the peat range from 3.5 m to 4 m. The lithologic units that occur on the traverse are silt sand, sandy clay, peat and silt clay.

The radar facies that characterize the third traverse are F5, F4, F3 and F2 (Figure 11). The depth to the water table on is 0 m. The depth of the peat layer ranges from 6 m to 6.5 m and the thickness of the peat ranges from 3 m to 3.5 m. The lithologic units that occur on the traverse are silt sand, sandy clay, peat and silt clay.

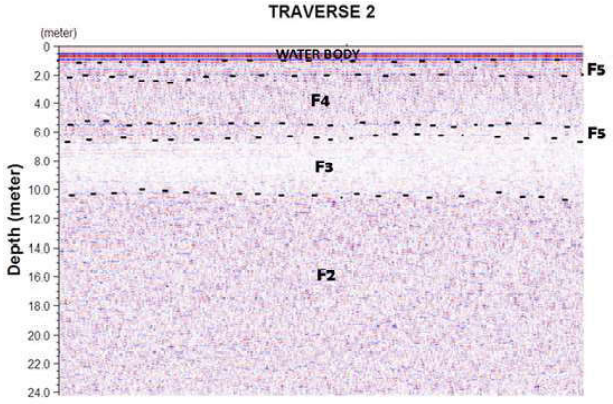

Figure 10: Radar facies for Traverse 2

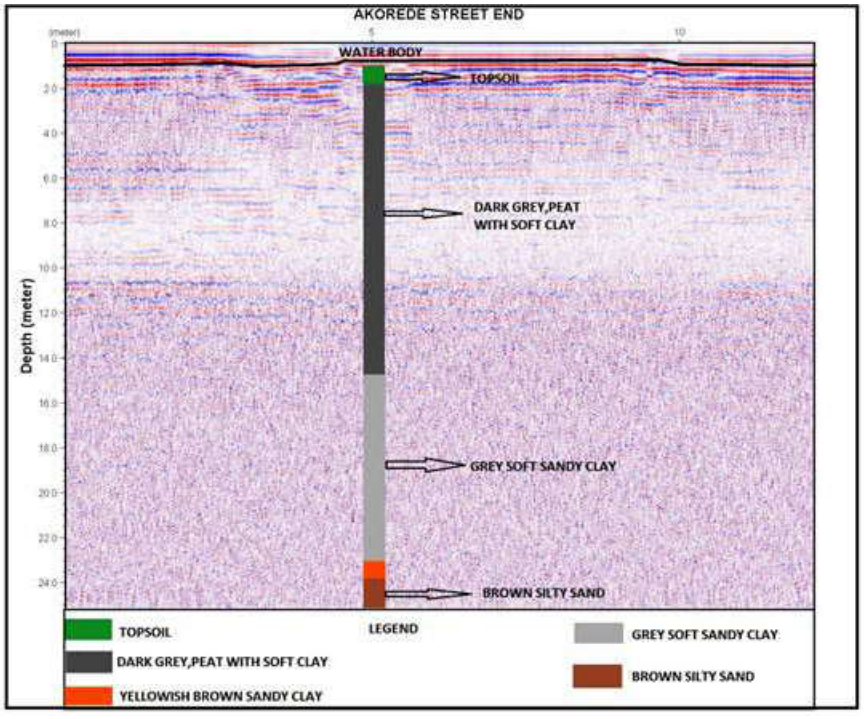

Figure 9: Correlation of radar facies and BH 03

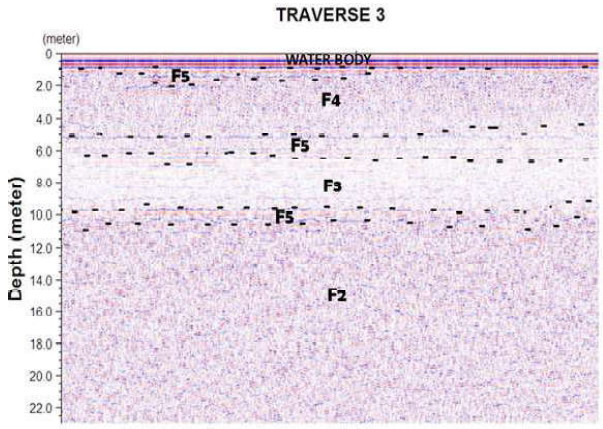

Figure 11: Radar facies for Traverse 3

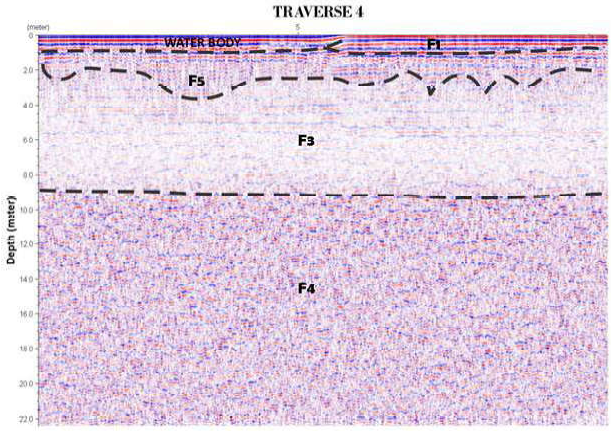

Figure 12: Radar facies for Traverse 4

The radar facies that characterize the fourth traverse are F1, F3, F4 and F5 (Figure 12). The depth to the water table on is 0 m. The depth of the peat layer ranges from 2 m to 3 m and the thickness of the peat range from 10 m to 11 m. Clay intercalations occur within the peat layer. The lithologic units that occur on the traverse are topsoil, peat, sandy clay and silt sand. A borehole (BH 05) was drilled along the traverse and the result of the log interpretation is presented in Figure 13.

The GPR stratigraphy obtained at chainage point Ch.750m (Figure 14) reveals relatively thin parallel to sub-parallel, horizontal reflections with good continuity which is interpreted as top soil/sand-filled layer; the study area is marshy and so various portions have been sand-filled to enable accessibility. The water table exists just beneath this layer. The topsoil is absent on the portion of the traverse run on water and is replaced by the refuse- and litter-ridden water column. The topsoil is underlain by a layer with high amplitude, sinuous, horizontal, chaotic, moderately continuous reflections. This layer interpreted as silt-sand has thickness varying from 0.8 to 4.5 m. Low amplitude (almost reflection-free) planar, moderately continuous reflections with a thickness of 3.5 to 7 m underlay the silt-sand unit.

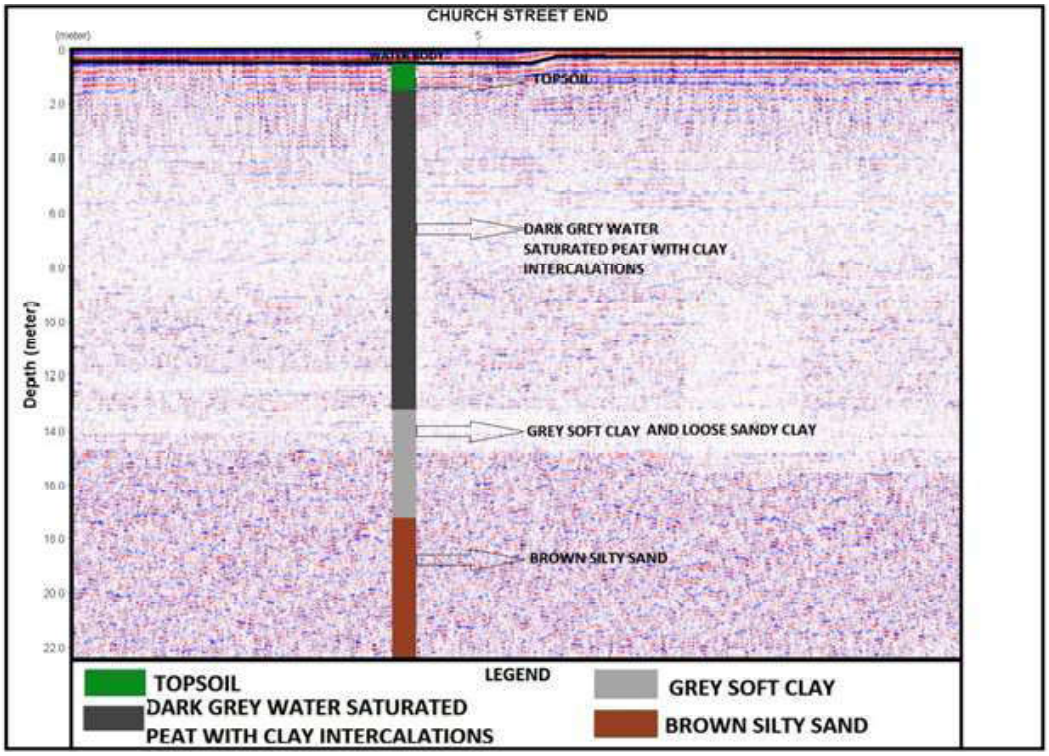

Figure 13: Correlation of radar facies and BH 05

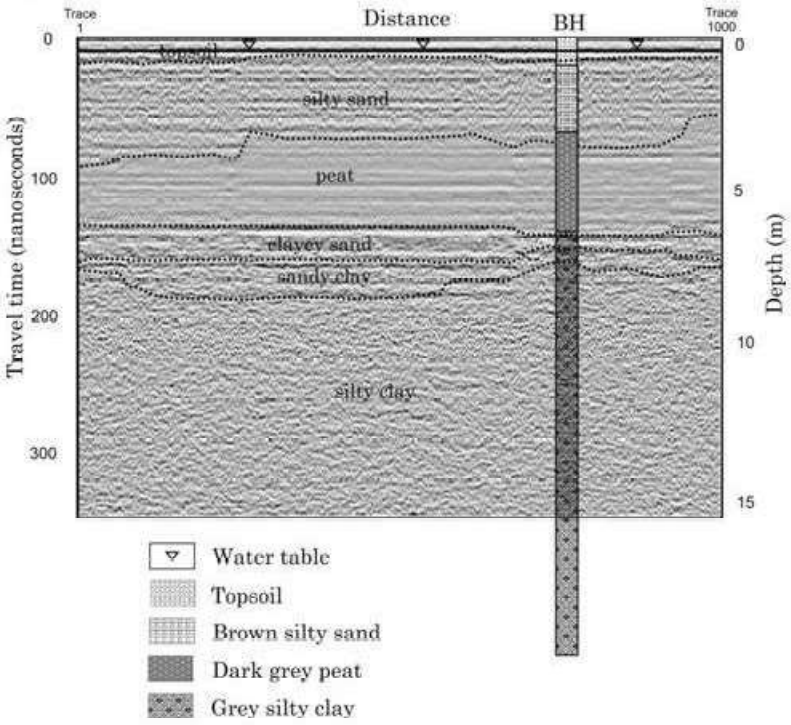

Figure 14: GPR Reflection at Ch.750m (North – South direction)

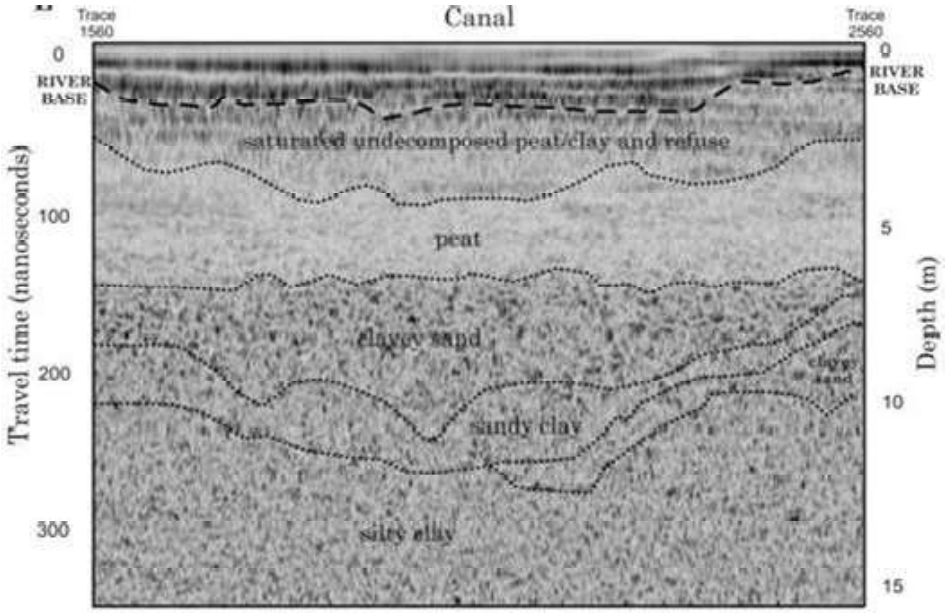

Figure 15: GPR Reflection at Ch.900m (North – South direction)

This is the layer of interest (peat) and the depth of occurrence ranges from 1.5 m to 9 m along the traverse. Moderate to high amplitude, planar, horizontal, sub-parallel reflections which became more prominent on approaching the river underlay the peat layer. This sandy/clayey layer had a marked boundary with the overlying peat, although the radar image showed a gradual transition between these sandy/clayey layers. A thick sequence of discontinuous chaotic reflections with high amplitude and sinuous configuration interpreted as silt-sand underlie the sandy/clayey unit.

The GPR stratigraphy obtained at chainage point Ch. 900m (Figure 15) showed similarity to Ch.1000m. The geometry of the river bed was clearly shown on the GPR section and the river base had a maximum depth of 3.5 m. Domestic waste such as refuse, sewage and plants were seen on the river and such materials were held in suspension in the water. Furthermore, part of these had settled to

the base as undecomposed peat/clay and waste with thickness range of 1 to 2 m. This layer directly overlay the peat which has similar geometry with that seen along Ch.750 m. The clayey-sand layer beneath the peat unit had straddled in it, sandy clay units in places, showing a gradual change in thickness and geometry of the clayey/sandy layer from land to water. The shallow-occurring silt-clay unit on land was seen to occur much deeper at 10 m (Figure 15).

The GPR stratigraphy obtained at chainage point Ch.1000 m showed similarity to Ch.900 m, but for the presence of sedimentary structures (ripples marks) within the peat (Figure 16), which is indicators of the transportation medium and paleo-current direction of the peat. As indicated by the ripple marks, the peat was possibly deposited in fluvial environment with the N-S direction of flow.

The boreholes logs obtained in the study area were correlated across four of the GPR traverses (Figure 17). Also, 3D cubes which show the spatial and lateral extent of the peat layer were produced from the combination of the 2D GPR sections obtained in the study area. This is presented in Figures 18 to 20.

The results of the depth to the water-Bed measurements taken on the field are shown below as two-dimensional (2D) and three-dimensional (3D) plots. Assuming the water level on land is at 0 datum, while the top to the depth of the canal floor from about (275 m - (end of traverse) ranges from (0 - to 2 m).

4.0 Conclusion

The GPR data acquired in the study area revealed the presence of five distinct radar facies namely; topsoil, silt clay, peat, sandy clay and silt sand. The stratigraphic unit of interest, peat, was correlated across the eight GPR traverses studied and revealed the peat layer has varying thickness from 3 m to 11 m in the subsurface. The depth of occurrence of the peat also ranged from 1.5 m to 6 m. An obvious decrease in depth to the peat vis-à-vis peat thicknesses from Ch.625 m to Ch.1100 m was obtained.

In addition, correlation of the results of the GPR data with the borehole log suites obtained in the area showed similarities in depth and thickness of the peat bogs. Furthermore, an attempt was made to infer the in-situ geophysical and elastic properties of the peat from the GPR data. The derived parameters from the GPR studies shows that the Peat found in the investigated area at Badia are fibrous peat with low strength, medium to low bedding stress and high volumetric water content (VWC).

High resolution Ground Penetrating Radar and hydrographic survey have revealed the general geometry and architecture, sedimentary units and patterns existing in the Badia Canal area of Lagos. Good correlation exists between the geophysical properties estimated from the GPR data and the field data obtained.

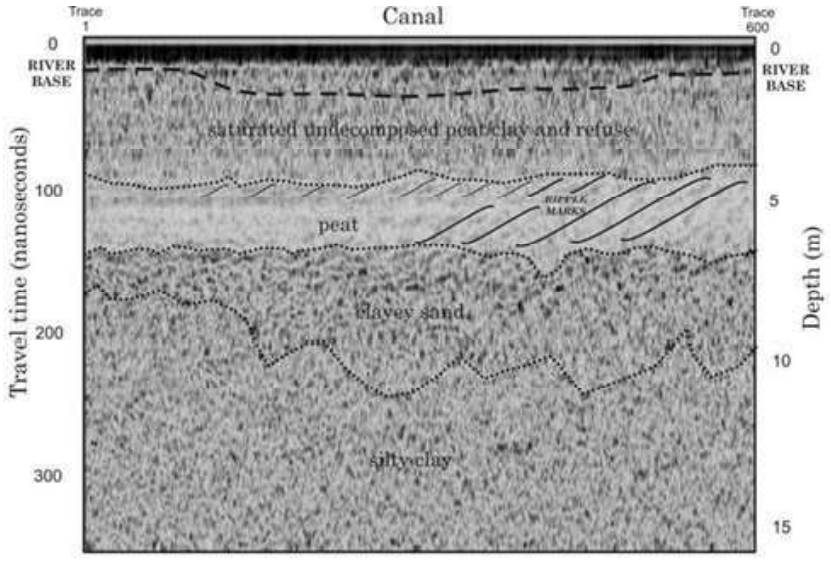

Figure 16: GPR Reflection at Ch.1000m (North – South direction)

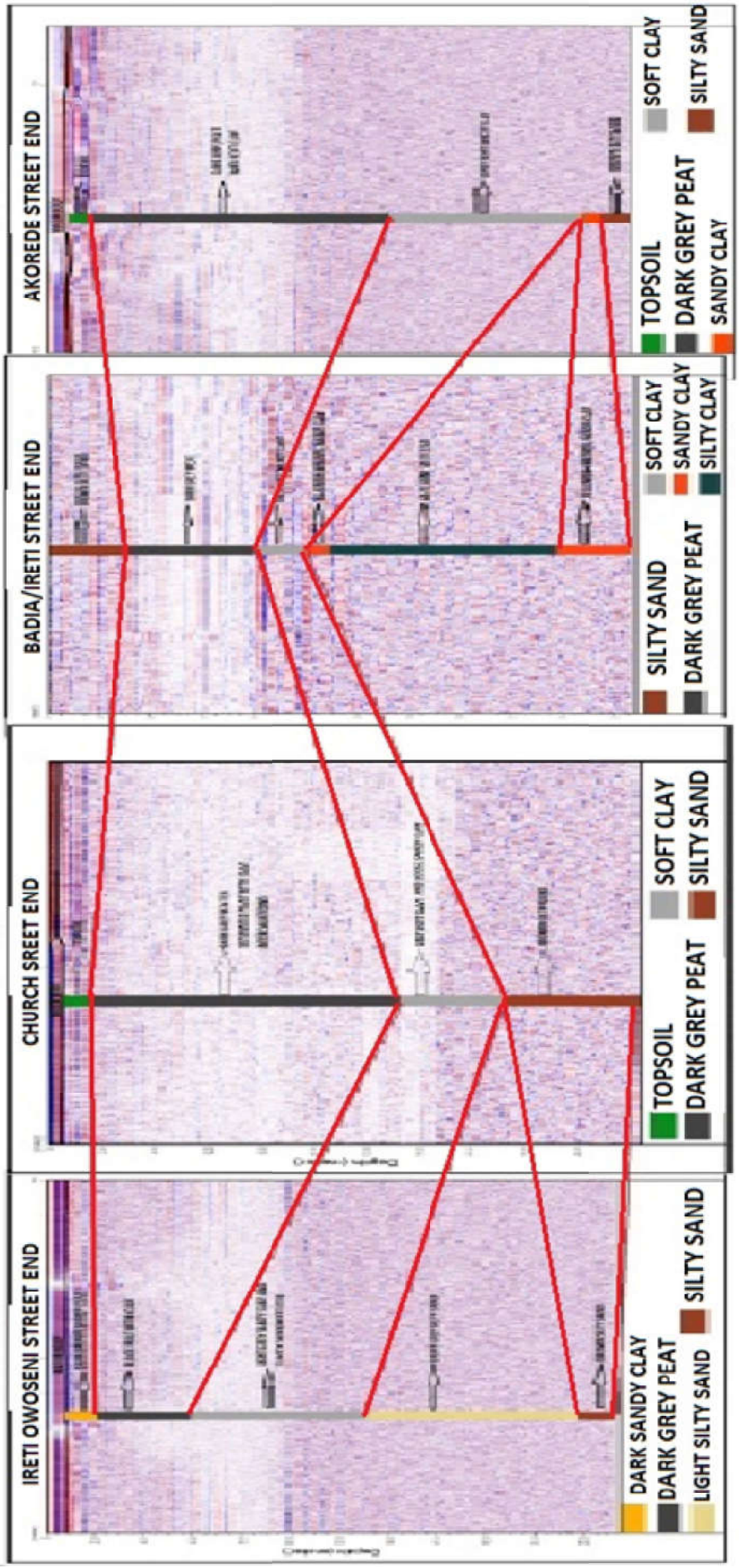

Figure 17: Correlation of the four borehole logs with the GPR facies

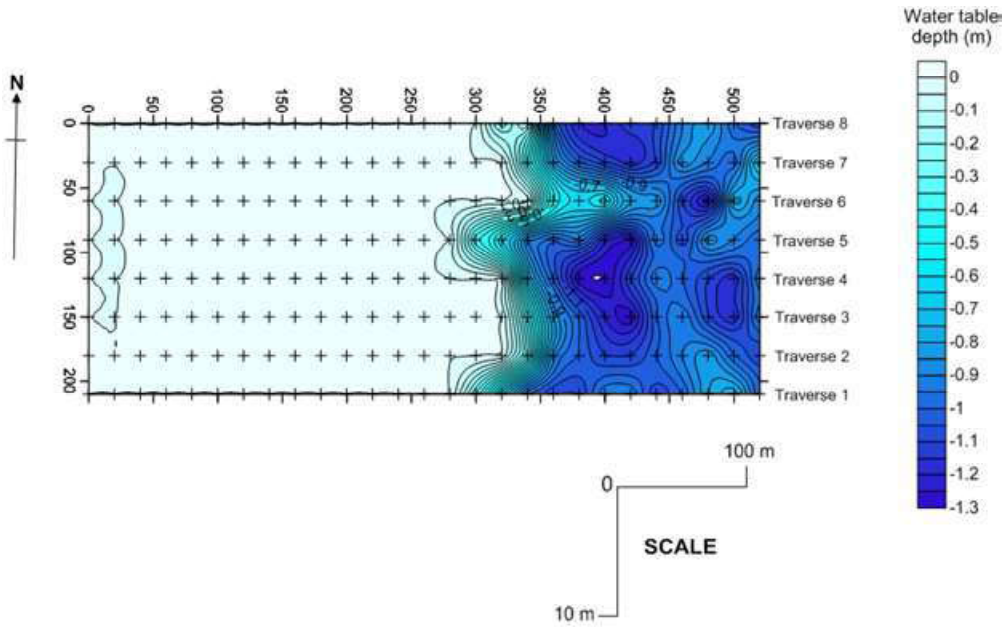

Figure 18: 2D representation of the depth to water table in the study area

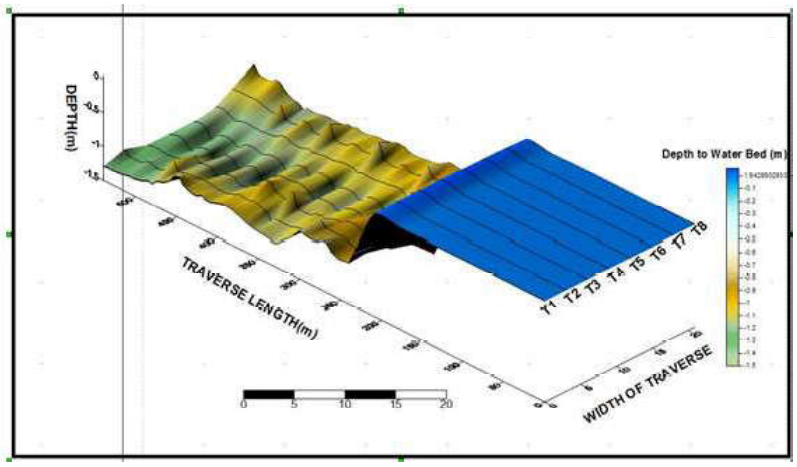

Figure 19: 3D representation of the depth to water table in the study area

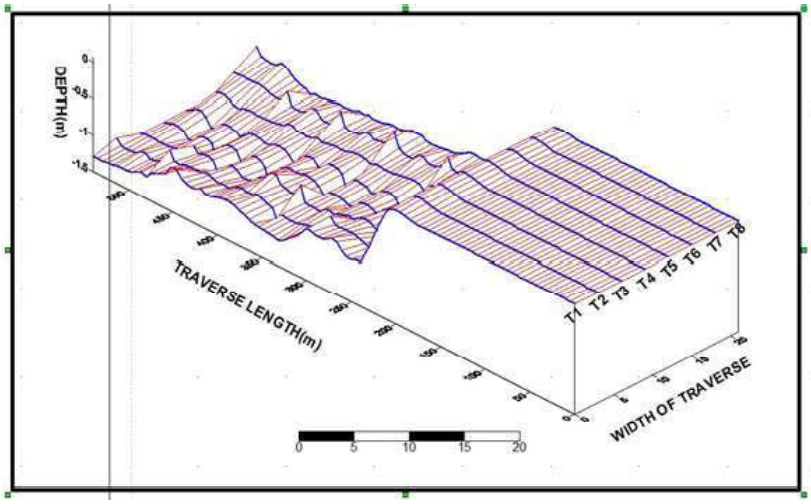

Figure 20: 3D wireframe representation of the depth to water table in the study area

Acknowledgement
The authors acknowledge the contributing institutions

References

Agagu O.A., 1985, A Geology guide to the bituminous sediments in southwestern Nigeria. Published by the Geol. Dept. University of Ibadan. 12 p.

Annan, A. P. 2002, The History of Ground Penetrating Radar. Subsurface Sensing Technologies and Applications, **3,** 303 – 320.

Apapa Local Government 2002, Planning Information on Badia: A Blighted Area.

Conyers, L. B., 2015, "Ground Penetrating Radar Data Analysis for More Complete Archaeological Interpretations". Pol. 53, pp. 202-207

Doolittle, J.A., 2013, "Technical Report on EMI and Saline Seep Workshop, Great Falls". USDA-NRCS-National Soil Survey Center, Lincoln, Nebraska, pp. 18–27

Doolittle, J.A., Windhorn, R.D., Withers, D.L., Zwicker, S.E., Heisner, F.E., McLeese, B.L., 2008, "Soil scientists revisit a high-intensity soil survey in Northwest Illinois with electromagnetic induction and tradition methods". Soil Surv. Horiz. **49 (4),** 102–108.

Durotoye, A. B. 1975, "Quaternary sediments in Nigeria" (C.A. Kogbe edited). Geology of Nigeria, Elisabeth Press, Lagos, pp.431-451.

Goodman, D. and Piro, S. 2013, "Ground Penetrating Radar Remote Sensing in Archaeology", Geotechnologies and the Environment, Springer Science: New York, NY, USA, Vol.9.

Huat, B. K., Asadi, A and Kazemian, S. 2009, "Experimental investigation of Geomechanical properties of Tropical Organic Soils and Peat". American Journal of Engineering and Applied Sciences **2 (1),** 184-188.

Jones, H.A and Hockey, R. D 1964, "The Geology of part of Southwestern Nigeria", Geological Survey of Nigeria, Bulletin 31, pp. 10-34.

Leggo, P. J. and Leech, C. 1983, "Surbsurface investigations for shallow mine workings and cavities by the ground impulse radar technique". Ground Engineering, **16:** 20-23.

Leuschen C. J. and Plumb R. G. 2001, "A matched filter based reverse time migration algorithm for ground penetrating radar". IEEE Transactions on Geoscience and Remote Sensing, 39 (5), 929-936.

Longe, E.O., Malomo, S., and Olorunniwo, M.A. 1987, "Hydrogeology of Lagos metropolis", Journal of African Earth Sciences, 6**(3),** 163-174.

Mitchum, R. M.., Vail, P. R., and Sangree, J. B. 1977, Stratigraphic interpretation of seismic reflection patterns in depositional sequences. In: Payton, C. E. (Ed), Seismic Stratigraphy-Applications to Hydrocarbon Exploration. AAPG Mem. **16,** 117-123.

Neal, A. 2004, "Ground Penetrating Radar and its Use in Sedimentology: Principles, Problems, and Progress". Earth Science Review, **66,** 261-330.

Olabode S. O. and Mohammed M. Z. 2016, "Depositional Facies and Sequence Stratigraphic Study in Parts of Benin (Dahomey) Basin SW Nigeria: Implications on the Re-Interpretation of Tertiary Sedimentary Successions", International Journal of Geosciences, **7,** 210-228.

Oldenburg, D. W. and Pratt, D. A. 2007, "Geophysical Inversion for Mineral Exploration: a Decade of Progress in Theory and Practice", Proceedings of Exploration 07: Fifth Decennial International Conference on Mineral Exploration, p. 61-95

Patterson, J. E. 2001, "Application of Ground Penetrating Radar (GPR) at the cryo-genie gem pegmatite mine,San Diego County, California, University of Calgary.

Saharudin, M. A., Nordina M. M., Nordina A. N. and Maslinda U. 2016, "Application of Ground Penetrating Radar in Detecting Target of Interest". International Research Journal of Engineering and Technology, **3(1),** 48-53.

Takahashi, K., Preetz, H. and Igel J. 2011, "Soil properties and performance of landmine detection by metal detector and ground penetrating radar – soil characterisation and its verification by a field test". Journal of Applied Geophysics, Elsevier, **73(4),** 368-377.

Timo, S. and Pekka, M. 2011, "The Use of Ground Penetrating Radar in Road Rehabilitation Projects". Roadscanners Oy, Finland.

Van Dam, R.L., Van den Berg, E. H., Shaap, M. G., Broekema, L. H., and Schalger, W. 2003, "Radar Reflections from Sedimentary Structures Zone, In: Ground Penetrating Radar in Sediments, Bristow, C. S. and Jol, H. M. (Eds.). Geol. Soc. Geological Sociwty of London, USA., 257-273.